Magnetic-Field-Modulated Resonant Tunneling in Ferromagnetic-Insulator-Nonmagnetic Junctions

Yang Song[1,*] and Hanan Dery[1,2]
[1]Department of Electrical and Computer Engineering, University of Rochester, Rochester 14627, New York, USA
[2]Department of Physics and Astronomy, University of Rochester, Rochester 14627, New York, USA
(Received 18 February 2014; published 25 July 2014)

We present a theory for resonance-tunneling magnetoresistance (MR) in ferromagnetic-insulator-nonmagnetic junctions. The theory sheds light on many of the recent electrical spin injection experiments, suggesting that this MR effect rather than spin accumulation in the nonmagnetic channel corresponds to the electrically detected signal. We quantify the dependence of the tunnel current on the magnetic field by quantum rate equations derived from the Anderson impurity model, with the important addition of impurity spin interactions. Considering the on-site Coulomb correlation, the MR effect is caused by competition between the field, spin interactions, and coupling to the magnetic lead. By extending the theory, we present a basis for operation of novel nanometer-size memories.

DOI: 10.1103/PhysRevLett.113.047205 PACS numbers: 85.75.Mm, 73.40.Gk, 85.30.Mn

Spintronics applications essentially rely on injection, manipulation, and detection of spins [1]. Demonstrations of electrically injected spin accumulation in nonmagnetic materials are considered reliable when measured in a nonlocal geometry [2,3]. In this setup, shown in Fig. 1(a), one ferromagnetic electrode injects or extracts spin-polarized electrons and a second one detects the spin accumulation of electrons (V_{NL}) that diffuse outside the path of a constant charge current (I_T). Because the spin diffusion length of many nonmagnetic materials is in the $\lesssim 1$ μm range, it is advantageous to have a submicron separation between the injector and detector electrodes [4–6]. To mitigate this requirement, many researchers have recently resorted to a local measurement wherein one ferromagnetic electrode is used for both injection and detection of the spin signal [V in Fig. 1(a)] [7–22]. Figure 1(b) shows the typically observed change in the detected resistance when applying an external magnetic field. Similar to the Hanle-type experiment of optical spin injection [1,23–25], the width and amplitude of the Lorentzian-shaped signal (ΔB and ΔR) are frequently used to extract the spin lifetime and accumulation density. A critical problem, however, is that standard spin diffusion and relaxation theories cannot explain many of the recent local-setup experiments. First, ΔR is too large to account for spin accumulation. Second, ΔB and ΔR are surprisingly insensitive to which nonmagnetic material is employed, while ΔB is oddly comparable for electrons and holes. These facts raise big questions on the underlying physics, especially in technologically relevant materials such as silicon.

In this Letter, we present a theory for resonance-tunneling magnetoresistance (MR) in ferromagnetic-insulator-nonmagnetic (F-I-N) junctions. We explain the greatly enhanced spin signals in numerous local spin injection and detection setups, showing that ΔB and ΔR do not depend on spin accumulation and relaxation in the nonmagnetic material. As the detector junction remains unbiased only for the nonlocal setup, the local detection is highly prone to impurity-assisted tunnel current. We propose that those enhanced signals and their dependence on temperature are set by impurities with large on-site Coulomb repulsion compared with the voltage bias. Depending on the electron occupation of the resonance level, the MR effect is established by the interplay between the Zeeman energy and the impurity coupling to the ferromagnetic material. Considering molecular fields due to spin-spin interactions such as hyperfine and exchange, we capture the origin of ΔB and the sign dependence of the signal on magnetic field orientation. Last but not least, by extending the theory to tunneling in one-dimensional (1D)

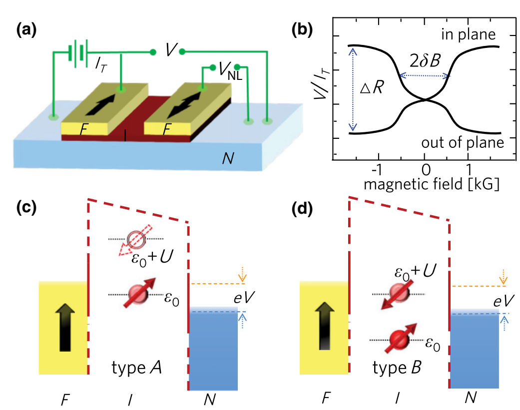

FIG. 1 (color online). (a) Nonlocal and local electrical setups for detecting spin accumulation. (b) The measured signal $\delta R(B) = [V(B) - V(0)]/I_T$ is a change in junction resistance when applying in-plane or out-of-plane magnetic fields. The Lorentzian due to the in-plane field is typically observed only in the local setup. Resonant tunneling via (c) type A or (d) type B impurities for spin injection (electrons flow from F to N).

 © 2014 American Physical Society

structures, we set forth a framework for a novel type of nanometer-size tunnel memory.

To quantify the MR, we tailor the Anderson impurity model to the tunneling problem with spin polarized leads [26,27]. The system Hamiltonian for the $s = \frac{1}{2}$ impurity reads

$$H = \sum_{\ell \mathbf{k}\sigma} [\varepsilon_{\ell \mathbf{k}\sigma} a^\dagger_{\ell \mathbf{k}\sigma} a_{\ell \mathbf{k}\sigma} + (T_{\ell\sigma} a^\dagger_{\ell \mathbf{k}\sigma} d_\sigma + \text{H.c.})] + U n_\uparrow n_\downarrow + \varepsilon_\uparrow(\theta) n_\uparrow + \varepsilon_\downarrow(\theta) n_\downarrow + \varepsilon_B \sin\theta (d^\dagger_\uparrow d_\downarrow + d^\dagger_\downarrow d_\uparrow). \quad (1)$$

The energy of an electron with wave vector $\mathbf{k}$ and spin σ in the ℓth lead (F or N) is denoted $\varepsilon_{\ell\mathbf{k}\sigma}$. The creation (annihilation) Fermi operators in the lead and impurity are defined by $a^\dagger_{\ell\mathbf{k}\sigma}$ ($a_{\ell\mathbf{k}\sigma}$) and $d^\dagger_\sigma$ (d_σ), respectively. The interaction between the lead and impurity is denoted by $T_{\ell\sigma}$, assumed here to be $\mathbf{k}$ independent for simplicity. The on-site Coulomb interaction between electrons of opposite spins is denoted by U and $n_\sigma = d^\dagger_\sigma d_\sigma$. The $\sigma = \uparrow(\downarrow)$ component is parallel to the majority (minority) spin population of the ferromagnetic material. The second line in Eq. (1) denotes the impurity Zeeman terms where θ is the angle between $\mathbf{B}$ and the spin quantization direction. $\varepsilon_{\uparrow,\downarrow}(\theta) = \epsilon_0 \pm \varepsilon_B \cos\theta$, where ϵ_0 is the resonance energy of the singly occupied state and $\varepsilon_B = g\mu B/2$. The off-diagonal terms $d^\dagger_\sigma d_{\bar\sigma}$ result from spin precession.

We briefly describe the derivation of the resonance current. The equation of motion for density-matrix operators is

$$\begin{aligned} -i\hbar \frac{d}{dt} d^\dagger_\sigma d_{\sigma'} &= [H, d^\dagger_\sigma d_{\sigma'}] \\ &= \sum_{\ell,\mathbf{k}} T_{\ell\sigma} a^\dagger_{\ell\mathbf{k}\sigma} d_{\sigma'} - T_{\ell\sigma'} d^\dagger_\sigma a_{\ell\mathbf{k}\sigma'} \\ &\quad + \varepsilon_B \sin\theta (d^\dagger_{\bar\sigma} d_{\sigma'} - d^\dagger_\sigma d_{\bar\sigma'}) \\ &\quad \pm 2\varepsilon_B \cos\theta d^\dagger_\sigma d_{\sigma'} \delta_{\bar\sigma\sigma'}. \end{aligned} \quad (2)$$

Henceforth, the + (−) sign refers to the case that $\sigma = \uparrow$ ($\downarrow$). To form a closed equation set, we use the Langreth theorem and recast the averages of the sum terms into lesser and retarded Green functions on the impurity [28–30]

$$\sum_{\ell,\mathbf{k}} T_{\ell\sigma} \langle a^\dagger_{\ell\mathbf{k}\sigma} d_{\sigma'} \rangle = \sum_\ell \int \frac{d\varepsilon}{2\pi} \Gamma_{\ell\sigma} \left(G^R_{\sigma'\sigma} f_{\ell\sigma} + \frac{1}{2} G^<_{\sigma'\sigma} \right). \quad (3)$$

$f_{\ell\sigma}(\varepsilon)$ is the Fermi distribution of the σ spin in the ℓth lead and $\Gamma_{\ell\sigma}(\varepsilon) = 2\pi \sum_{\mathbf{k}} |T_{\ell\sigma}|^2 \delta(\varepsilon - \varepsilon_{\ell\mathbf{k}\sigma})$ is its coupling to the impurity. The analysis is greatly simplified outside the Kondo regime and by assuming weak coupling ($\Gamma \ll \{k_B T, eV\}$). We focus on two impurity types wherein the population of the resonance state fluctuates between zero and one [type A, see Fig. 1(c)] or between one and two electrons [type B, see Fig. 1(d)]. This classification is motivated by the dependence of the Green functions on the impurity population. It is justified when considering together the broad energy distribution of midgap impurity defects at oxide tunnel barriers [37–41] and the large on-site Coulomb repulsion U. Under the common conditions of local-setup experiments $eV \gg k_B T \gg \varepsilon_B$, we can replace $f_{\ell\sigma}(\varepsilon)$ by 1 (0) for the injector (extractor) lead, and the Green functions take simple forms in Eq. (3) where $\Gamma(\varepsilon)$ varies slowly on the scale of ε_B (e.g., $\int_{eV} d\varepsilon G^<_{\sigma'\sigma} = 2i\pi(\langle n_\uparrow \rangle + \langle n_\downarrow \rangle - 1)\delta_{\sigma\sigma'}$ for type B impurity; see the Supplemental Material [30] for details). The analysis becomes independent of spin accumulation in the leads. Putting these pieces together, we reach a concise equation set [30,42–44]. For spin extraction via type A impurities [electrons flow from N to F, opposite to the spin-injection bias setting in Fig. 1(c)],

$$\begin{aligned} \hbar \dot n_{\sigma\sigma} &= \Gamma_N P_0 - (1 \pm p)\Gamma_F n_{\sigma\sigma} - 2\varepsilon_B \sin\theta \,\mathrm{Im}(n_{\bar\sigma\sigma}), \\ \hbar \dot n_{\sigma\bar\sigma} &= i\varepsilon_B[\sin\theta(n_{\bar\sigma\bar\sigma} - n_{\sigma\sigma}) \pm 2\cos\theta n_{\sigma\bar\sigma}] - \Gamma_F n_{\sigma\bar\sigma}, \end{aligned} \quad (4)$$

where $n_{\sigma\sigma'} \equiv \langle d^\dagger_\sigma d_{\sigma'} \rangle$. $P_0 = 1 - n_{\uparrow\uparrow} - n_{\downarrow\downarrow}$ is the probability for zero occupation and the coupling parameters $\Gamma_\ell(\varepsilon) = (\Gamma_{\ell\uparrow} + \Gamma_{\ell\downarrow})/2$ are evaluated around the impurity's energy level ϵ_0. The interface current polarization is given by $p = (\Gamma_{F\uparrow} - \Gamma_{F\downarrow})/2\Gamma_F$ [1]. The master equations for injection conditions are obtained by exchanging $\Gamma_{N\sigma} \equiv \Gamma_N$ with $\Gamma_{F\sigma}$. Similarly, the equations for type B impurities are obtained by evaluating $\Gamma_{F(N)}$ around $\epsilon_0 + U$, by considering double rather than zero occupancy ($P_2 = n_{\uparrow\uparrow} + n_{\downarrow\downarrow} - 1$), and by noting that type A and B impurities flip roles in extraction and injection conditions [30]. This feature reflects their symmetry and can be viewed as electron (hole) tunneling across type A (B) impurities [45].

The resonance currents are found from the steady state solution of the master equations using $i_A = 2e\Gamma_N P_0/\hbar$ and $i_B = e\Gamma_N(1 - P_2)/\hbar$ for extraction, or $i_A = -e\Gamma_N(1 - P_0)/\hbar$ and $i_B = -2e\Gamma_N P_2/\hbar$ for injection [they implicitly relate to $\Gamma_{F\sigma} n_{\sigma\sigma}$ by Eq. (4)]. For $eV \gg k_B T$, we get [30]

$$\begin{aligned} i_A^{N\to F} &= -i_B^{F\to N} = \frac{2e}{\hbar} \frac{\Gamma_F \Gamma_N}{2\Gamma_N + \Gamma_F} \frac{1 - p^2\chi(\mathbf{B})}{1 - \alpha p^2 \chi(\mathbf{B})}, \\ i_B^{N\to F} &= -i_A^{F\to N} = \frac{2e}{\hbar} \frac{\Gamma_F \Gamma_N}{2\Gamma_F + \Gamma_N}, \\ \chi(\mathbf{B}) &= \frac{B_F^2 + B^2\cos^2\theta}{B_F^2 + B^2}, \quad \alpha = \frac{\Gamma_F}{2\Gamma_N + \Gamma_F}, \quad B_F = \frac{\Gamma_F}{g\mu_B}. \end{aligned} \quad (5)$$

Most relevant to our analysis, the resonance current across type A and B impurities depends on the magnetic field in extraction and injection conditions, respectively [via $\chi(\mathbf{B})$]. This dependence is best perceived when considering half-metallic F and an out-of-plane magnetic field ($p = 1$ and $\theta = \pi/2$). Without a magnetic field, extraction via type A impurity or injection via type B impurity is completely blocked, $i_A^{N\to F} = i_B^{F\to N} = 0$. In extraction via type A impurity, electrons tunnel from the nonmagnetic material into the impurity and have equal probability to be parallel or antiparallel to the spin orientation in the half metal. The tunnel conductance is blocked once an antiparallel spin settles on the impurity. For injection via type B impurity we get that once the lower impurity level is filled with an electron from the half metal, the upper resonant level can only accept the electron of opposite spin, which the half metal cannot provide. In a large out-of-plane field, the blockade is completely lifted in both cases due to depolarization of the impurity spin (Larmor precession). Finally, from Eq. (5) we get that $i_A + i_B$ merely flips sign when reversing the bias direction. Therefore, the MR effect in injection ($F \to N$) and extraction ($N \to F$) is similar if the densities of type A and B impurities are similar.

To compare the analysis with experimental findings we incorporate important extensions on the effective magnetic field at the impurity site. When comprised of the external field alone, $\mathbf{B} = \mathbf{B}_e$, the modulation amplitude $\Delta i(\theta_e) = i(B_e \gg B_F) - i(B_F \gg B_e)$ is

$$\Delta i(\theta_e) = \frac{\sin^2\theta_e}{1 - \alpha p^2 \cos^2\theta_e} \frac{(1-\alpha)p^2}{1 - \alpha p^2} i_0, \tag{6}$$

where $i_0 = 2\alpha e \Gamma_N / \hbar$. Throughout this work, $\mathbf{B}_e$ is assumed smaller than the out-of-plane coercive field of F. We see that the MR effect vanishes for an in-plane external field ($\theta_e = 0$) in contrast to most measurements where the in-plane field modulation is larger than that of the out of plane case. Furthermore, for $\mathbf{B} = \mathbf{B}_e$ the signal width stems from the coupling to F ($\Delta B \sim B_F$), thereby decreasing exponentially with increasing oxide thickness. In virtually all local-setup measurements of F-I-N structures, on the other hand, $\Delta B \sim 0.1$–1 kG regardless of the oxide details [7–20]. To explain these aforementioned observations, we examine the ubiquitous spin interactions, which tend to randomize the spin orientation at the impurities. They include, for example, hyperfine fields due to interaction with the nuclear spins and exchange interactions between nearby impurities. Invoking the mean-field approximation, an effective internal magnetic field can be written by $\mathbf{B}_i = \mathbf{B}_{\rm hf} + \mathbf{B}_{ex} = (\langle A\mathbf{I}\rangle + \langle J_{nn}\mathbf{S}\rangle)/g\mu_B$ where A is the hyperfine coupling constant with nuclear spin $\mathbf{I}$ and J_{nn} is the exchange coupling with an electron of spin $\mathbf{S}$ on the nearest neighbor impurity. Considering ferromagnet-oxide-silicon as a case study, unpaired electrons on ^{29}Si dangling bonds would experience hyperfine fields of a few hundred gauss [39,40,46–48]. Similar defects can exist in Al_2O_3 barriers [41,49–51] or perovskite interfaces [52]. The defect densities can be controlled by oxide preparation techniques [20]. The sources for $\mathbf{B}_i$ also include stray fields whose amplitude and direction depend on the interface roughness [12].

With $\mathbf{B} = \mathbf{B}_e + \mathbf{B}_i$, we can complete the analysis using Eq. (5) and write the extraction (injection) tunnel current via a type A (B) impurity, $i = i_A = -i_B$,

$$\frac{i}{i_0} = 1 - (1-\alpha)p^2 \int dB_i \int d\cos\theta_i \times \int d\phi_i \frac{B_\parallel^2 \mathcal{F}(B_i, \theta_i, \phi_i)}{B_\perp^2 + (1-\alpha p^2) B_\parallel^2}. \tag{7}$$

i is averaged over $\mathcal{F}(B_i, \theta_i, \phi_i)$, the normalized distribution for the internal field. The components of the effective field along and normal to F are $B_\parallel^2 = B_F^2 + (B_{i\parallel} + B_{e\parallel})^2$ and $B_\perp^2 = B_{i\perp}^2 + B_{e\perp}^2 + 2B_{i\perp}B_{e\perp}\cos(\phi_i - \phi_e)$, respectively. Figures 2(a) and 2(b) show the solution of Eq. (7) with hyperfine fields of common defect centers in Si-oxide interfaces. The tunneling involves unpaired electrons on ^{29}Si dangling bonds next to the oxygen vacancy V_0 in the barrier (E' center) or in the Si_3 configuration on the atomic interface (P_d center). The hyperfine field of E' is assumed isotropic with amplitude of 420 G [46], and that of P_d has axial symmetry with an out-of-plane (in-plane) amplitude of 160 G (90 G) [48]. Figure 2(c) shows the solution for internal fields due to exchange between nearest-neighbor impurities. The localization length and impurity density in the tunnel barrier are chosen as $\ell_i = 4.4$ Å and $n_i = 8 \times 10^{18}$ cm^{-3}, respectively. Further details are provided in the Supplemental Material [30]. In all three cases we assume $\langle B_i \rangle > B_F$ so that the width of the signal is set by internal fields rather than by coupling with F (i.e., ΔB is essentially independent of barrier thickness). The modulation amplitude in the regime that $B_i \gg B_F$ is realized from $\Delta i(\theta_e) = i(B_e \gg B_i) - i(B_i \gg B_e)$. For an isotropic internal field distribution $[\mathcal{F}(B_i, \theta_i, \phi_i) = \mathcal{F}(B_i)/4\pi]$,

$$\Delta i(\theta_e) = \frac{1-\alpha}{\alpha}\left[\frac{\operatorname{arctanh}(\sqrt{\alpha}p)}{\sqrt{\alpha}p} - \frac{1}{1 - \alpha p^2 \cos^2\theta_e}\right] i_0. \tag{8}$$

The in-plane field modulation can exceed that of the out-of-plane field and increases for internal fields that point mostly in the out-of-plane direction [e.g., $|\Delta i(0)/\Delta i(\pi/2)| > n + 2$ when $\mathcal{F} \propto \sin^n\theta_i \mathcal{F}(B_i)$].

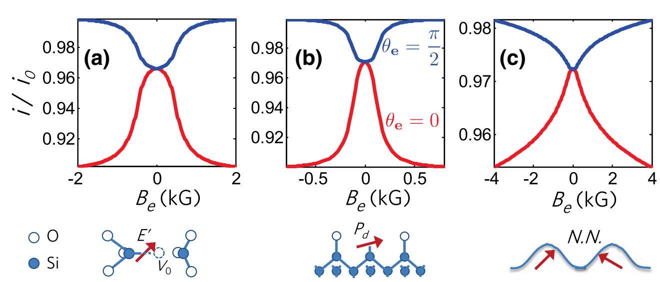

FIG. 2 (color online). Calculated MR via an impurity with $\alpha = 0.1$ embedded in the F-I-N junction with $p = 1/3$. MR due to resonant tunneling via an (a) E' and (b) P_d defect in silicon-oxide interfaces. (c) MR in the presence of molecular fields due to exchange between nearest-neighbor impurities.

We can now quantify the total voltage change that one measures in the local geometry [ΔR in Fig. 1(b)]. Denoting the total tunneling current used in experiments [Fig. 1(a)] as I_T, for small MR effect we simply have

$$\frac{\Delta R}{R} = \sum_n \frac{\Delta i_n(0) - \Delta i_n(\frac{\pi}{2})}{I_T} = \frac{1}{I_T} \sum_n \frac{(1-\alpha_n)p^2}{1-\alpha_n p^2} i_{0,n}, \quad (9)$$

where n runs over type A (B) impurities in the tunnel barrier for spin extraction (injection). The much larger total current is by tunneling via larger impurity clusters for which $U \lesssim eV$ and via background direct tunneling. The MR effect is enabled by the nonzero polarization of a F-I-N junction ($p \neq 0$), rendering it distinct from resonant tunneling MR in N-I-N junctions where $g\mu B > \{k_B T, eV\}$ [37,45]. Since ΔR measures the effect at the $B_e \gg \{B_i, B_F\}$ limit, its amplitude is robust and independent of the details of the internal field distribution. Accordingly, one can use either Eq. (6) or (8) to get Eq. (9). The amplitude of $\Delta R/R$ depends on the junction's polarization, the impurities' density and their coupling to the leads (via α and i_0).

Discussion.—The MR effect in F-I-N junctions comes from electron spin precession in impurities whose population fluctuates between 0 and 1 (type A) when electrons flow into F, or between 1 and 2 (type B) when electrons flow from F. The resonance current through these impurities is suppressed or enabled when applying in-plane or out-of-plane magnetic fields, respectively. The physics is explained by reinforcement or removal of the Pauli blockade in the respective field configurations.

The MR effect is stronger for impurities located closer to the nonmagnetic than to the ferromagnetic material ($\Gamma_N \gg \Gamma_F$ so $\alpha \to 0$). This physics is understood by noting that when electrons flow into (from) F, type A (B) impurities are mostly empty (doubly occupied) if they are closer to F. Therefore, spin precession becomes meaningless and the modulation is not observed. The disappearance of the effect for $\alpha \to 1$ also explains the results in a recent comprehensive experimental analysis of F-I-semiconductor junctions [53]. A strong suppression in the MR signal is found when the oxide thickness decreases (exponential increase of Γ_F), unlike the total R that for ultrathin oxides is governed by the Schottky barrier (Γ_N). This physics also sets apart the measurements of F-I-semiconductor junctions from those with direct F-semiconductor contacts [21,25,30,54]. In the latter case, the true signal from spin accumulation in N cannot be masked by the presence of impurities at the atomic interface between F and the semiconductor for which $\Gamma_F \gg \Gamma_N$.

Thus far we have treated the on-site Coulomb repulsion as the largest energy scale $U \gg eV$ (when the MR is most effective). Now we invoke the relation between U and various sizes of impurity clusters in order to explain the nontrivial bias (V) and temperature (T) dependencies of the MR signal. We note that U is smaller for relatively large clusters due to their reduced charging capacitance, and that the effective size of a cluster grows with T due to the thermally activated crosstalk between adjacent impurities [55]. The T dependence typically follows the Arrhenius law with an activation energy E_a that depends on disorder density and impurity type [56]. Thus, as $k_B T$ rises above the corresponding E_a such that for the resulting impurity cluster $U \lesssim eV$, this particular cluster stops affecting the MR. This interplay between U and eV, and between $k_B T$ and E_a resolves the strong dependence of $\Delta R(T)$ signals found in several recent experiments [7,8,13,19]. At small bias V, the relevant E_a for threshold $U_{\rm th} \approx eV$ is small as it corresponds to large and dense clusters, and as a result the MR effect is more susceptible to temperature at the low T region $k_B T \approx E_a$. At large bias, on the other hand, the relevant E_a becomes larger as the MR is from the outset limited to isolated point defects (largest U), for which the T dependence is weaker ($k_B T \ll E_a$).

The proposed analysis solves two additional important problems in electrical spin injection. First, it addresses the observed signals in local-setup experiments where the net charge current across the tunnel junction is zero but where the bias voltage is distributed (i.e., spin injection and extraction in different parts of the junction) [57]. So far, the measured signals in such experimental settings were attributed to the spin Seebeck effect in spite of a similar orders-of-magnitude discrepancy with the theory of spin injection [30]. Second, the proposed mechanism supports the fact that the measured MR effect is independent of doping type in F-I-semiconductor junctions [7,11,19]. We have seen that the expected signal does not depend on spin relaxation in N, and therefore a comparable effect is expected in both n- and p-type semiconductors. The original attribution to spin relaxation in N, on the other hand, contradicts known physics of the ultrashort (subpicosecond) spin lifetime in hole bands [30,58–60].

Outlook.—The MR mechanism can be generalized beyond spin injection with ferromagnetic leads. Figure 3 shows such an example for a 1D nanometer-size memory cell that utilizes A-B impurity chains. Recent measurements in N-I-N tunnel junctions show that A-B chains result in a similar MR effect, where the type A impurity serves as an effective one-electron source with its polarization susceptible to weak magnetic fields [56]. A sufficient external field turns off the current by reinforcing the Pauli blockade across the A-B chain [56]. As shown in Figs. 3(a) and 3(b), the "0" and "1" states are defined by the position of an unpaired electron embedded in an insulator adjacent to the A-B chain. Its position is controlled by the writing voltage V_W. The exchange interaction with the embedded electron when positioned in the "1" state sets the effective internal magnetic field ($B_{\rm ex}$) exerted on the type B impurity. The readout is enabled by the MR effect across the A-B chain as shown in Fig. 3(c). Note that confinement of the applied magnetic field

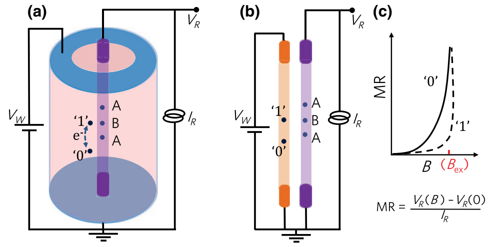

FIG. 3 (color online). Nano-size tunnel memory relying on the MR effect. (a) The basic cell is a 1D conducting nanowire in an insulator (e.g., DXP molecules in zeolites [61]), or adjacent insulating and conducting wires as shown in (b). In either configuration, the writing voltage (V_W) sets the position of an unpaired electron in one of two impurities embedded in the insulator (labeled '1' and '0'). The conducting wire includes a critical *A*-*B*-*A* impurity chain which becomes Pauli blocked when applying a magnetic field [56]. (c) The MR effect facilitates the information readout due to its strong dependence on the exchange field of the unpaired electron (see text).

is not needed since the spin does not encode information. Once the challenge for atomic-level lithographic control is met, this architecture represents the ultimate scaling of memories since "it leaves no room in the bottom."

We are indebted to Felix Casanova, Oihana Txoperena, Kohei Hamaya, and Ian Appelbaum for insightful discussions and for sharing invaluable data prior to their publication. This work is supported by NRI-NSF, NSF, and DTRA Contracts No. DMR-1124601, No. ECCS-1231570, and No. HDTRA1-13-1-0013, respectively.

*yangsong@pas.rochester.edu

[1] I. Žutić, J. Fabian, and S. Das Sarma, Rev. Mod. Phys. **76**, 323 (2004).
[2] M. Johnson and R. H. Silsbee, Phys. Rev. B **35**, 4959 (1987).
[3] F. J. Jedema, A. T. Filip, and B. J. van Wees, Nature (London) **410**, 345 (2001).
[4] Y. Ji, A. Hoffmann, J. E. Pearson, and S. D. Bader, Appl. Phys. Lett. **88**, 052509 (2006).
[5] F. Casanova, A. Sharoni, M. Erekhinsky, and I. K. Schuller, Phys. Rev. B **79**, 184415 (2009).
[6] T. Sasaki, T. Oikawa, M. Shiraishi, Y. Suzuki, and K. Noguchi, Appl. Phys. Lett. **98**, 012508 (2011).
[7] S. P. Dash, S. Sharma, R. S. Patel, M. P. de Jong, and R. Jansen, Nature (London) **462**, 491 (2009).
[8] M. Tran, H. Jaffrés, C. Deranlot, J.-M. George, A. Fert, A. Miard, and A. Lemaître, Phys. Rev. Lett. **102**, 036601 (2009).
[9] C. H. Li, O. M. J. van 't Erve, and B. T. Jonker, Nat. Commun. **2**, 245 (2011).
[10] K.-R. Jeon, B.-C. Min, Y.-H. Park, H.-S. Lee, C.-Y. Park, Y.-H. Jo, and S.-C. Shin, Appl. Phys. Lett. **99**, 162106 (2011).
[11] N. W. Gray and A. Tiwari, Appl. Phys. Lett. **98**, 102112 (2011).
[12] S. P. Dash, S. Sharma, J. C. Le Breton, J. Peiro, H. Jaffrés, J.-M. George, A. Lemaître, and R. Jansen, Phys. Rev. B **84**, 054410 (2011).
[13] A. Jain *et al.*, Phys. Rev. Lett. **109**, 106603 (2012).
[14] O. M. J. van 't Erve, A. L. Friedman, E. Cobas, C. H. Li, J. T. Robinson, and B. T. Jonker, Nat. Nanotechnol. **7**, 737 (2012).
[15] Y. Aoki, M. Kameno, Y. Ando, E. Shikoh, Y. Suzuki, T. Shinjo, M. Shiraishi, T. Sasaki, T. Oikawa, and T. Suzuki, Phys. Rev. B **86**, 081201(R) (2012).
[16] T. Uemura, K. Kondo, J. Fujisawa, K.-I. Matsuda, and M. Yamamoto, Appl. Phys. Lett. **101**, 132411 (2012).
[17] W. Han, X. Jiang, A. Kajdos, S.-H. Yang, S. Stemmer, and S. S. P. Parkin, Nat. Commun. **4**, 2134 (2013).
[18] K.-R. Jeon, B.-C. Min, Y.-H. Park, S.-Y. Park, and S.-C. Shin, Phys. Rev. B **87**, 195311 (2013).
[19] Y. Pu, J. Beardsley, P. M. Odenthal, A. G. Swartz, R. K. Kawakami, P. C. Hammel, E. Johnston-Halperin, J. Sinova, and J. P. Pelz, Appl. Phys. Lett. **103**, 012402 (2013).
[20] O. Txoperena, M. Gobbi, A. Bedoya-Pinto, F. Golmar, X. Sun, L. E. Hueso, and F. Casanova, Appl. Phys. Lett. **102**, 192406 (2013).
[21] Y. Ando, Y. Maeda, K. Kasahara, S. Yamada, K. Masaki, Y. Hoshi, K. Sawano, K. Izunome, A. Sakai, M. Miyao, and K. Hamaya, Appl. Phys. Lett. **99**, 132511 (2011).
[22] M. Ishikawa, H. Sugiyama, T. Inokuchi, K. Hamaya, and Y. Saito, Appl. Phys. Lett. **100**, 252404 (2012).
[23] W. Hanle, Z. Phys. **30**, 93 (1924).
[24] M. I. Dyakonov and V. I. Perel, in *Optical Orientation*, edited by F. Meier and B. P. Zakharchenya (North-Holland, New York, 1984), Vol. 8, pp. 15–71.
[25] X. Lou, C. Adelmann, M. Furis, S. A. Crooker, C. J. Palmstrøm, and P. A. Crowell, Phys. Rev. Lett. **96**, 176603 (2006).
[26] P. W. Anderson, Phys. Rev. **124**, 41 (1961).
[27] J. A. Appelbaum and D. R. Penn, Phys. Rev. **188**, 874 (1969).
[28] D. C. Langreth, in *Linear and Nonlinear Electron Transport in Solids*, edited by J. T. Devreese and V. E. Van Doren, Nato Advanced Study Institute, Series B: Physics, Vol. 17 (Plenum, New York, 1976).
[29] Y. Meir and N. S. Wingreen, Phys. Rev. Lett. **68**, 2512 (1992).
[30] See Supplemental Material at http://link.aps.org/supplemental/10.1103/PhysRevLett.113.047205 for the derivation of Eqs. (3), (4), and (7), quantitative approximations we adopt, and detailed discussions for local setup measurements, which includes Refs. [31–36].
[31] D. N. Zubarev, Usp. Fiz. Nauk **71**, 71 (1960) [Sov. Phys. Usp. **3**, 320 (1960)].
[32] C. Lacroix, J. Phys. F **11**, 2389 (1981).
[33] C. Herring and M. Flicker, Phys. Rev. **134**, A362 (1964).
[34] J. Kondo, Prog. Theor. Phys. **32**, 37 (1964).
[35] J. Appelbaum, Phys. Rev. Lett. **17**, 91 (1966).
[36] J. R. Schrieffer and P. A. Wolff, Phys. Rev. **149**, 491 (1966).
[37] D. Ephron, M. R. Beasley, H. Bahlouli, and K. A. Matveev, Phys. Rev. B **49**, 2989(R) (1994).
[38] H. Bahlouli, K. A. Matveev, D. Ephron, and M . R. Beasley, Phys. Rev. B **49**, 14496 (1994).

[39] M. Boero, A. Pasquarello, J. Sarnthein, and R. Car, Phys. Rev. Lett. **78**, 887 (1997).
[40] Z.-Y. Lu, C. J. Nicklaw, D. M. Fleetwood, R. D. Schrimpf, and S. T. Pantelides, Phys. Rev. Lett. **89**, 285505 (2002).
[41] W. H. Rippard, A. C. Perrella, F. J. Albert, and R. A. Buhrman, Phys. Rev. Lett. **88**, 046805 (2002).
[42] B. Dong, H. L. Cui, and X. L. Lei, Phys. Rev. B **69**, 035324 (2004).
[43] M. Braun, J. König, and J. Martinek, Phys. Rev. B **70**, 195345 (2004).
[44] S. A. Gurvitz and Y. S. Prager, Phys. Rev. B **53**, 15932 (1996).
[45] L. I. Glazman and K. A. Matveev, Pis'ma Zh. Eksp. Teor. Fiz. **48**, 403 (1988) [JETP Lett. **48**, 445 (1988)].
[46] D. L. Griscom, Phys. Rev. B **20**, 1823 (1979).
[47] M. G. Jani, R. B. Bossoli, and L. E. Halliburton, Phys. Rev. B **27**, 2285 (1983).
[48] K. L. Brower, Appl. Phys. Lett. **43**, 1111 (1983).
[49] A. Stashans, E. Kotomin, and J.-L. Calais, Phys. Rev. B **49**, 14854 (1994).
[50] H. Momida, S. Nigo, G. Kido, and T. Ohno, Appl. Phys. Lett. **98**, 042102 (2011).
[51] M. Choi, A. Janotti, and C. G. Van de Walle, J. Appl. Phys. **113**, 044501 (2013).
[52] R. Pentcheva and W. E. Pickett, Phys. Rev. B **74**, 035112 (2006).
[53] S. Sharma, A. Spiesser, S. P. Dash, S. Iba, S. Watanabe, B. J. van Wees, H. Saito, S. Yuasa, and R. Jansen, Phys. Rev. B **89**, 075301 (2014).
[54] M. K. Chan, Q. O. Hu, J. Zhang, T. Kondo, C. J. Palmstrøm, and P. A. Crowell, Phys. Rev. B **80**, 161206(R) (2009).
[55] J. S. Helman and B. Abeles, Phys. Rev. Lett. **37**, 1429 (1976).
[56] O. Txoperena, Y. Song, L. Qing, M. Gobbi, L. E. Hueso, H. Dery, and F. Casanova, arXiv:1404.0633.
[57] J.-C. Le Breton, S. Sharma, H. Saito, S. Yuasa, and R. Jansen, Nature (London) **475**, 82 (2011).
[58] D. J. Hilton and C. L. Tang, Phys. Rev. Lett. **89**, 146601 (2002).
[59] E. J. Loren, J. Rioux, C. Lange, J. E. Sipe, H. M. van Driel, and A. L. Smirl, Phys. Rev. B **84**, 214307 (2011).
[60] F. Pezzoli, F. Bottegoni, D. Trivedi, F. Ciccacci, A. Giorgioni, P. Li, S. Cecchi, E. Grilli, Y. Song, M. Guzzi, H. Dery, and G. Isella, Phys. Rev. Lett. **108**, 156603 (2012).
[61] R. N. Mahato, H. Lülf, M. H. Siekman, S. P. Kersten, P. A. Bobbert, M. P. de Jong, L. De Cola, and W. G. van der Wiel, Science **341**, 257 (2013).